Scientia Iranica, Vol. 9, No. 4, pp 346-353

SCIENTIA
IRANICA

Dynamic Interactions of Multiple Multi-Functional UPFC in Power Systems

M. Jazaeri[1], M. Ehsan*, H.F. Wang[1] and A.T. Johns[1]

In this paper, a systematic method is presented for modeling a multi-machine power system with multiple UPFC's installed and the dynamic interaction between different control functions of the UPFCs is investigated. Study undertaken on New England power systems demonstrates that the existence of dynamic interaction may lead to the instability of the whole system.

INTRODUCTION

A Unified Power Flow Controller (UPFC) [1] is a multi-functional FACTS (Flexible AC Transmission System) controller with the primary function of power flow control plus some secondary functions [2-5]. To implement the multiple control functions of the UPFC, it is suggested that multiple controllers are used in the UPFC, with each of them being designed for a single control function [4]. However, arrangement of multiple controllers to implement multiple control functions poses the problem of possible dynamic interaction, not only between the control functions of a single UPFC (local interaction) but also between different UPFCs (inter-device interaction) [6]. In [6], it has been shown that such interactions exist between two UPFCs installed in a simple single-machine, infinite-bus power system.

In this paper, it is demonstrated that, in a multi-machine power system, if the multiple UPFC controllers are designed separately, interaction can cause poor performance and, even, closed-loop control system instability when all controllers are in joint operation.

DYNAMIC MODEL

There are several models, which have been developed by different authors for a UPFC. A literature survey review on the modeling of a UPFC has been published by the authors [7]. Based on open literature, most of the papers have proposed a UPFC model for load flow studies, i.e, power injected models, and none of them modeled the UPFC internal dynamics except [8]. The UPFC model developed by [8] is adopted in this paper. This model is obviously more comprehensive than others for dynamic state studies, because the dynamics of the DC link capacitor is considered in the modeling process.

A UPFC consists of an Excitation Transformer (ET), a Boosting Transformer (BT), two three-phase GTO-based Voltage Source Converters (VSCs) and a DC link capacitor. In Figure 1, m_E, m_B, δ_E and δ_B refer to the amplitude modulation index and phase angle of the two VSC's in the UPFC, respectively. They are the input control signals of the UPFC closed-loop control system.

If the General Pulse Width Modulation (GPWM) is adopted for the GTO-based VSCs, by applying Park's transformation and ignoring the resistance and transients of the transformers, the dynamic model of

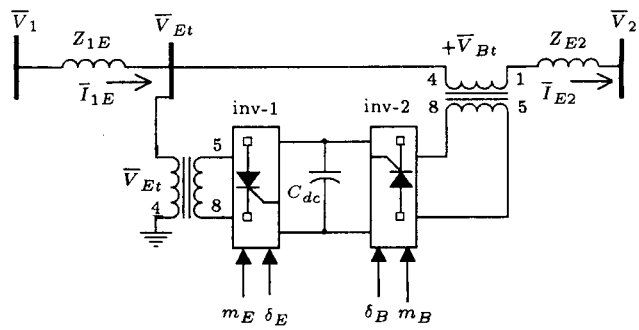

Figure 1. One line diagram of the UPFC installed between bus 1 and bus 2.

1. *Department of Electronics and Electrical Engineering, University of Bath, Bath BA2 7AY, UK.*
*. *Corresponding Author, Department of Electrical Engineering, Sharif University of Technology, Tehran, I.R. Iran.*

the UPFC can be established to be:

$$\frac{dv_{dc}}{dt} = -\frac{3m_E}{4C_{dc}}\begin{bmatrix}\cos\delta_E & \sin\delta_E\end{bmatrix}\begin{bmatrix}I_{Ed}\\ I_{Eq}\end{bmatrix} - \frac{3m_B}{4C_{dc}}\begin{bmatrix}\cos\delta_B & \sin\delta_B\end{bmatrix}\begin{bmatrix}I_{Bd}\\ I_{Bq}\end{bmatrix}, \quad (1)$$

$$\overline{V}_{Et} = jx_E\overline{I}_E + \overline{V}_E, \quad (2)$$

$$\overline{V}_{Bt} = jx_B\overline{I}_{E2} + \overline{V}_B, \quad (3)$$

where:

$$\overline{I}_E = \overline{I}_{1E} - \overline{I}_{E2},$$

$$\overline{V}_E = \frac{m_E v_{dc}}{2}e^{j\delta_E},$$

$$\overline{V}_B = \frac{m_B v_{dc}}{2}e^{j\delta_B}.$$

Controllers

UPFC installation in a power system is mainly for the active and reactive power flow control along the transmission line and AC voltage support at the UPFC shunt bus bar. Moreover, for the normal operation of the UPFC, DC voltage across the DC link capacitor needs to be controlled by a DC voltage regulator, such that active power exchanges between the UPFC and the power system is zero at the steady-state operation. If a Proportional plus Integral (PI) control scheme is used for the UPFC controllers [9], four UPFC control laws can be summarised as follows:

1. dc voltage regulation:

$$\delta_E = \delta_{E0} + (K_{p1} + K_{I1}/s).(V_{dcref} - V_{dcm}), \quad (4)$$

2. Active power flow control:

$$m_B = m_{B0} + (K_{p2} + K_{I2}/s).(P_{ref} - P_m), \quad (5)$$

3. AC bus voltage control:

$$m_E = m_{E0} + (K_{p3} + K_{I3}/s).(V_{acref} - V_{acm}), \quad (6)$$

4. Reactive power flow control:

$$\delta_B = \delta_{B0} + (K_{p4} + K_{I4}/s).(Q_{ref} - Q_m). \quad (7)$$

Fourth-Order Synchronous Machine Model

The fourth order model of a synchronous generator is chosen in this paper. The model, including the AVR's dynamics, is described by the following equations:

$$\dot{e}'_q = \frac{(E_{fd} - E_I)}{T'_{do}}, \quad (8)$$

$$\dot{e}'_d = \frac{-e'_d + (x_q - x'_q)I_{Gq}}{T'_{qo}}, \quad (9)$$

$$\dot{\delta} = \omega_0(\omega - 1), \quad (10)$$

$$\dot{\omega} = \frac{1}{2H}(P_m - P_e - D(\omega - 1)), \quad (11)$$

$$\dot{E}_{fd} = -\frac{E_{fd}}{T_A} + \frac{K_A}{T_A}(V_{tref} - V_t), \quad (12)$$

where $E_I = e'_q + (x_d - x'_d)I_{Gd}$ and, also, I_{Gd} and I_{Gq} are the d and q components of the generator current.

THE MODEL OF THE MULTI-MACHINE POWER SYSTEM INSTALLED WITH TWO UPFCS

To establish a non-linear dynamic model of a multi-machine power system with two UPFCs installed, the UPFC model must be embedded into the power system model. The systematic method proposed in [10] is extended in order to derive the non-linear dynamic model of two UPFCs installed in the multi-machine power system.

Assume a UPFC is installed on a transmission line, line 1-2 (line #1), as shown in Figure 2. The following circuit equations can, thus, be obtained:

$$\overline{V}_1 = Z_{1E}\overline{I}_{1E} + \overline{V}_{Et},$$

$$\overline{V}_{Et} = \overline{V}_{Bt} + Z_{E2}\overline{I}_{E2} + \overline{V}_2,$$

$$\overline{I}_E = \overline{I}_{1E} - \overline{I}_{E2}.$$

In matrix form, they become:

$$\begin{bmatrix}\overline{V}_1\\ \overline{V}_2\end{bmatrix} = \begin{bmatrix}Z_{1E} + jx_E & -jx_E\\ jx_E & -(Z_{E2} + jx_E + jx_B)\end{bmatrix}\begin{bmatrix}\overline{I}_{1E}\\ \overline{I}_{E2}\end{bmatrix} + \begin{bmatrix}1 & 0\\ 1 & -1\end{bmatrix}\begin{bmatrix}\overline{V}_E\\ \overline{V}_B\end{bmatrix}. \quad (13)$$

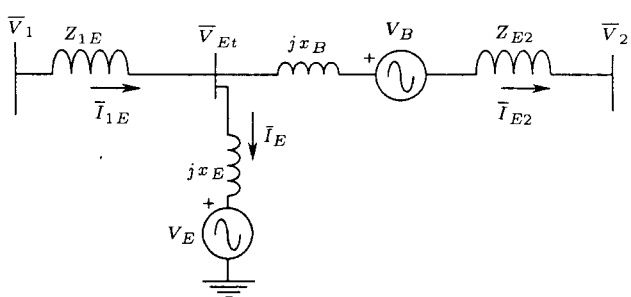

Figure 2. The circuit diagram of the UPFC installed in the transmission line.

For two UPFCs, installed on line #1 and line #2, Equation 13 can be modified to be:

$$\begin{bmatrix}\overline{V}_1\\ \overline{V}_2\\ \overline{V}_3\\ \overline{V}_4\end{bmatrix} = \begin{bmatrix}(Z_{1E}+jx_E) & -jx_E & 0 & 0\\ jx_E & -(Z_{E2}+jx_E+jx_B) & 0 & 0\\ 0 & 0 & (Z_{3E}+jxx_E) & -jxx_E\\ 0 & 0 & jxx_E & -(Z_{E4}+jxx_E+jxx_B)\end{bmatrix} \times \begin{bmatrix}\overline{I}_{1E}\\ \overline{I}_{E2}\\ \overline{I}_{3E}\\ \overline{I}_{E4}\end{bmatrix} + \begin{bmatrix}1 & 0 & 0 & 0\\ 1 & -1 & 0 & 0\\ 0 & 0 & 1 & 0\\ 0 & 0 & 1 & -1\end{bmatrix} \begin{bmatrix}\overline{V}_{E12}\\ \overline{V}_{B12}\\ \overline{V}_{E34}\\ \overline{V}_{B34}\end{bmatrix}. \quad (14)$$

In short form, it can be written as:

$$\overline{\mathbf{V}}_{1234} = \overline{\mathbf{A}}.\overline{\mathbf{I}}_{1E4} + \mathbf{B}.\overline{\mathbf{V}}_{EB12}$$

$$\Rightarrow \overline{\mathbf{I}}_{1E4} = \overline{\mathbf{A}}^{-1}.\overline{\mathbf{V}}_{1234} - \overline{\mathbf{A}}^{-1}.\mathbf{B}.\overline{\mathbf{V}}_{EB12}. \quad (15)$$

Also, before the UPFCs are installed, it can be assumed that the network admittance matrix is Y_r, where only n generator nodes, plus nodes 1 through 4, are kept:

$$\begin{bmatrix}\overline{y}_{11} & \overline{y}_{12} & \overline{y}_{13} & \overline{y}_{14} & \overline{\mathbf{Y}}_{15}\\ \overline{y}_{21} & \overline{y}_{22} & \overline{y}_{23} & \overline{y}_{24} & \overline{\mathbf{Y}}_{25}\\ \overline{y}_{31} & \overline{y}_{32} & \overline{y}_{33} & \overline{y}_{34} & \overline{\mathbf{Y}}_{35}\\ \overline{y}_{41} & \overline{y}_{42} & \overline{y}_{43} & \overline{y}_{44} & \overline{\mathbf{Y}}_{45}\\ \overline{\mathbf{Y}}_{51} & \overline{\mathbf{Y}}_{52} & \overline{\mathbf{Y}}_{53} & \overline{\mathbf{Y}}_{54} & \overline{\mathbf{Y}}_{55}\end{bmatrix} \begin{bmatrix}\overline{V}_1\\ \overline{V}_2\\ \overline{V}_3\\ \overline{V}_4\\ \overline{\mathbf{V}}_g\end{bmatrix} = \overline{\mathbf{Y}}_r. \begin{bmatrix}\overline{V}_1\\ \overline{V}_2\\ \overline{V}_3\\ \overline{V}_4\\ \overline{\mathbf{V}}_g\end{bmatrix} = \begin{bmatrix}0\\0\\0\\0\\\overline{\mathbf{I}}_g\end{bmatrix}. \quad (16)$$

With installation of UPFC1 on line #1 and UPFC2 on line #2, the network Equation 16 can be written as:

$$\begin{bmatrix}\overline{y}_{11}+\overline{y}_{12} & 0 & \overline{y}_{13} & \overline{y}_{14} & \overline{\mathbf{Y}}_{15}\\ 0 & \overline{y}_{22}+\overline{y}_{21} & \overline{y}_{23} & \overline{y}_{24} & \overline{\mathbf{Y}}_{25}\\ \overline{y}_{31} & \overline{y}_{32} & \overline{y}_{33}+\overline{y}_{34} & 0 & \overline{\mathbf{Y}}_{35}\\ \overline{y}_{41} & \overline{y}_{42} & 0 & \overline{y}_{44}+\overline{y}_{43} & \overline{\mathbf{Y}}_{45}\\ \overline{\mathbf{Y}}_{51} & \overline{\mathbf{Y}}_{52} & \overline{\mathbf{Y}}_{53} & \overline{\mathbf{Y}}_{54} & \overline{\mathbf{Y}}_{55}\end{bmatrix} \begin{bmatrix}\overline{V}_1\\ \overline{V}_2\\ \overline{V}_3\\ \overline{V}_4\\ \overline{\mathbf{V}}_g\end{bmatrix} + \begin{bmatrix}1 & 0 & 0 & 0\\ 0 & -1 & 0 & 0\\ 0 & 0 & 1 & 0\\ 0 & 0 & 0 & -1\\ \mathbf{0} & \mathbf{0} & \mathbf{0} & \mathbf{0}\end{bmatrix} \begin{bmatrix}\overline{I}_{1E}\\ \overline{I}_{E2}\\ \overline{I}_{3E}\\ \overline{I}_{E4}\end{bmatrix} = \begin{bmatrix}0\\0\\0\\0\\\overline{\mathbf{I}}_g\end{bmatrix} \quad (17)$$

By substituting Equation 15 into Equation 17 and making a partition to eliminate nodes 1 through 4 in Equation 17, it can be obtained that:

$$\begin{bmatrix}\overline{\mathbf{Y}}_1 & \vdots & \overline{\mathbf{Y}}_2\\ \cdots & \cdots & \cdots\\ \overline{\mathbf{Y}}_3 & \vdots & \overline{\mathbf{Y}}_4\end{bmatrix} \begin{bmatrix}\overline{\mathbf{V}}_{1234}\\ \cdots\\ \overline{\mathbf{V}}_g\end{bmatrix} + \begin{bmatrix}\mathbf{C}\\ \cdots\\ \mathbf{0}\end{bmatrix}.\left(\overline{\mathbf{A}}^{-1}.\overline{\mathbf{V}}_{1234} - \overline{\mathbf{A}}^{-1}.\mathbf{B}.\overline{\mathbf{V}}_{EB12}\right) = \begin{bmatrix}\mathbf{0}\\ \cdots\\ \overline{\mathbf{I}}_g\end{bmatrix}. \quad (18)$$

By using the Keron elimination method, nodes 1 through 4 can be deleted. Consequently, it is found that:

$$\overline{\mathbf{I}}_g = \overline{\mathbf{Y}}_g.\overline{\mathbf{V}}_g + \overline{\mathbf{Y}}_U.\overline{\mathbf{V}}_{EB12}, \quad (19)$$

where:

$$\overline{\mathbf{Y}}_g = \overline{\mathbf{Y}}_4 - \overline{\mathbf{Y}}_3.(\overline{\mathbf{Y}}_1 + \mathbf{C}.\overline{\mathbf{A}}^{-1})^{-1}.\overline{\mathbf{Y}}_2,$$

$$\overline{\mathbf{Y}}_U = -\overline{\mathbf{Y}}_3.(\overline{\mathbf{Y}}_1 + \mathbf{C}.\overline{\mathbf{A}}^{-1})^{-1}.\mathbf{C}.\overline{\mathbf{A}}^{-1}.\mathbf{B},$$

In Equation 19, $\overline{\mathbf{I}}_g$ and $\overline{\mathbf{V}}_g$ are expressed as a network reference frame. By applying the following transformation, the generator current can be expressed as a machine $d-q$ reference frame, presented as:

$$\overline{\mathbf{I}}_G = \mathbf{T}.\overline{\mathbf{I}}_g, \quad (20)$$

$$\overline{\mathbf{V}}_G = \mathbf{T}.\overline{\mathbf{V}}_g, \quad (21)$$

where:

$$\mathbf{T} = \text{diag.}\left[\begin{bmatrix}\sin\delta_i & -\cos\delta_i\\ \cos\delta_i & \sin\delta_i\end{bmatrix}\right].$$

Equations 1 and 8 to 12 give the full dynamic model of the multi-machine power system with two UPFCs installed.

CASE STUDY

Figure 3 shows the configuration of the New England Power System (NEPS).

The NEPS has 39 buses, 10 generators and 46 transmission lines and, in many studies, is considered to be a test power system. This paper has chosen the NEPS to investigate dynamic interaction between the control channels of two UPFCs installed on line #25 (L25) and line #23 (L23).

From the control theory point of view, if 8 controllers for two UPFCs are designed separately in

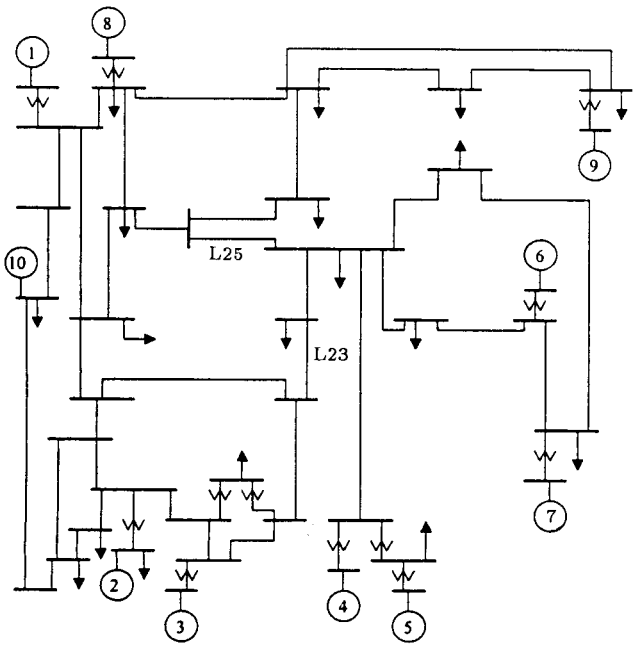

Figure 3. The New England test power system.

a sequence, the multiple functional UPFCs control is effectively treated as the SISO system. Inevitably, the dynamic interaction between the various control channels cannot be overcome. In this section, it is shown that the control performance and the closed-loop system stability cannot be guaranteed when these controllers are in joint operation, as they are supposed to, even though satisfactory control performance and closed-loop system stability are obtained when each controller is designed individually.

Eight PI-controllers are set individually and separately by the use of the standard tuning method for a PI controller design, which is carried out in the following sequence:

1) $PI - V_{dc1}$ controller is designed while all other controllers (7 controllers) are in open-loop. The tuned parameters are $K_{pdc1} = 10.0$ and $K_{Idc1} = 20.0$. Figure 4 shows the results of the non-linear simulation to assess controller performance. In the simulation, the reference DC voltage of the first UPFC, V_{dcref1}, is changed at 1.0 seconds of the simulation from 1.0 pu to 1.1 pu. From Figure 4, it can be seen that satisfactory control performance is achieved. Figure 5 shows the machine rotor angles (d), which confirm the stability of the closed-loop control system;
2) $PI - V_{Et1}$ is the second controller to be designed while all other controllers are open loop. The performance of this controller, with $K_{PV_{Et1}} = 0.5$ and $K_{IV_{Et1}} = 15.0$, is satisfactory, as shown by Figure 6 when its reference value (V_{Et1ref}) is increased by 0.01 pu. Figure 7 shows the machine angles, which are measured with respect to machine #10 angle position $[(\delta_i - \delta_{10})$ for $i = 1...9]$. It can be seen that the system is stable;
3) $PI - P_{line1}$ is the next controller to be designed while all other controllers are open loop. The controller performance, with $K_{PP_{line1}} = 0.05$ and

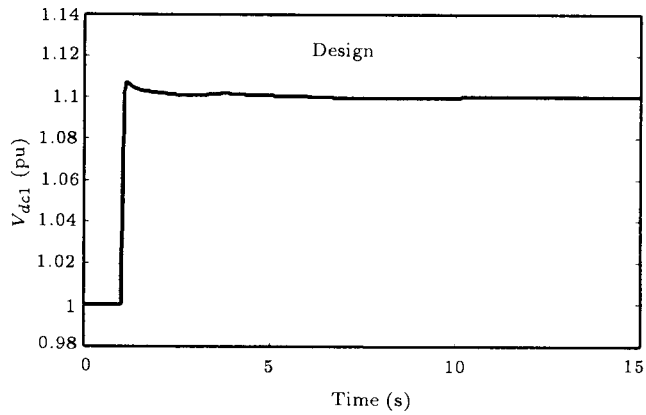

Figure 4. Step response of the system with $PI - V_{dc1}$ controller designed.

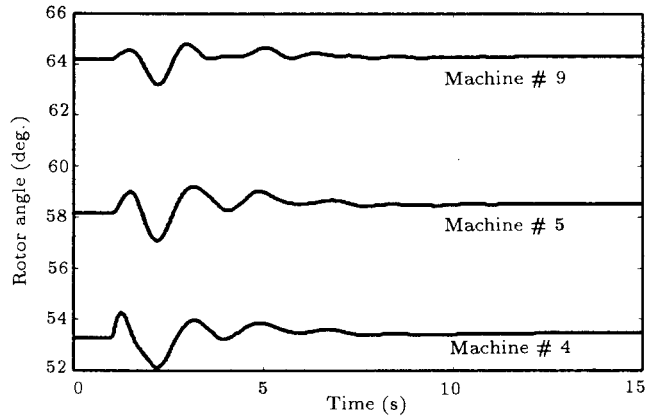

Figure 5. Rotor angle response of the system with $PI - V_{dc1}$ controller installed.

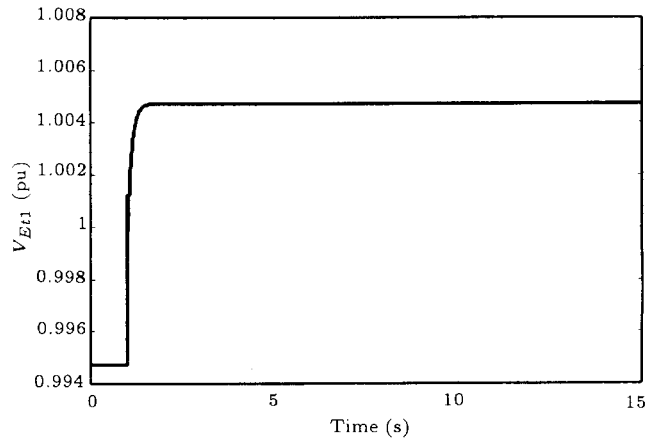

Figure 6. Step response of the system with $PI - V_{Et1}$ controller designed.

$K_{IP_{\text{line1}}} = 10.0$, is satisfactory when the reference value (P_{line1ref}) is changed, as shown in Figure 8. Figure 9 shows the machine angle's response;

4) $PI - Q_{\text{line1}}$ controller is the next controller to be designed with all other controllers out of service. The controller performance, with $K_{PQ_{\text{line1}}} = 0.8$ and $K_{IQ_{\text{line1}}} = 10.0$, is satisfactory when the reference value (Q_{line1ref}) is changed, as shown in Figure 10. Figure 11 shows the machine angle's response.

Four controllers in the second UPFC are designed individually and their performances are evaluated in the same way.

5) V_{dc2ref} is changed at 1.0 seconds from 1 pu to 1.1 pu with $K_{PV_{dc2}} = 10.5$ and $K_{IV_{dc2}} = 25.0$. Figures 12 and 13 show the system response;

6) V_{Et2ref} is changed at 1.0 seconds with $K_{PV_{Et2}} = 0.4$ and $K_{IV_{Et2}} = 13.0$. Figures 14 and 15 demonstrate the simulation results;

7) P_{line2ref} is changed at 1.0 second with $K_{PP_{\text{line2}}} = 1.0$ and $K_{IP_{\text{line2}}} = 16.1$. Figures 16 and 17 demonstrate the system response;

8) Q_{line2ref} is changed at 1.0 second with $K_{PQ_{\text{line2}}} = 0.1$

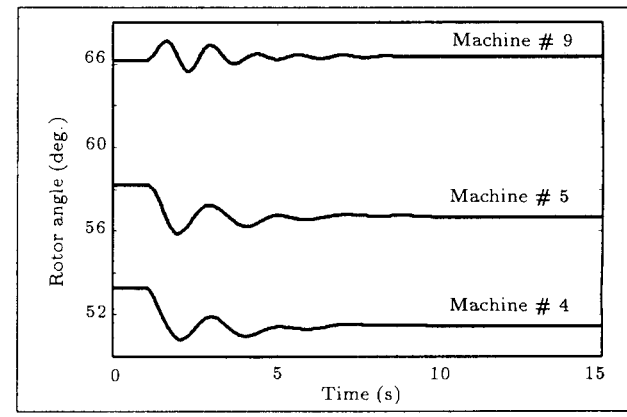

Figure 9. Rotor angle response of the system with $PI - P_1$ controller installed.

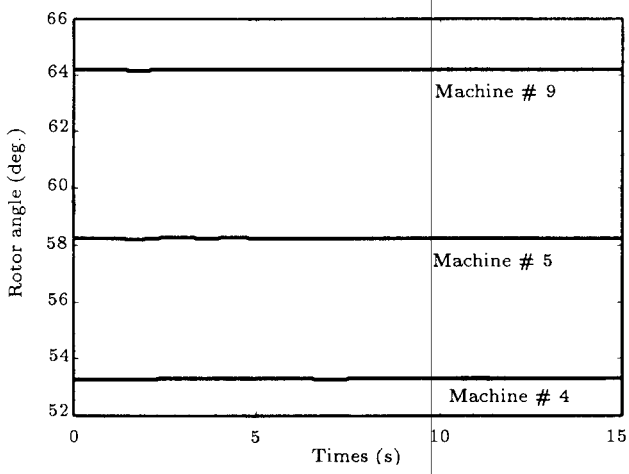

Figure 7. Rotor angle response of the system with $PI - V_{Et1}$ controller installed.

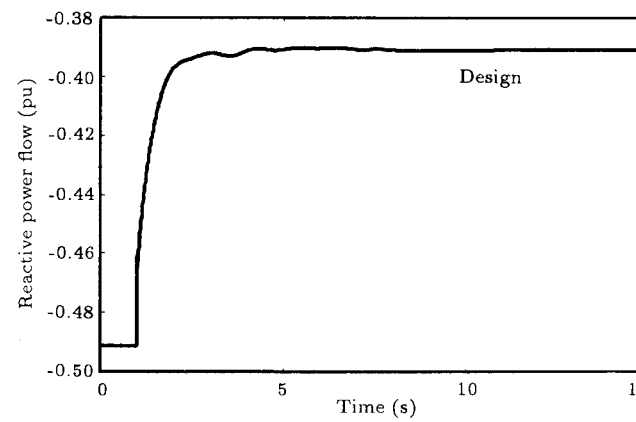

Figure 10. Step response of the system with $PI - Q_1$ controller designed.

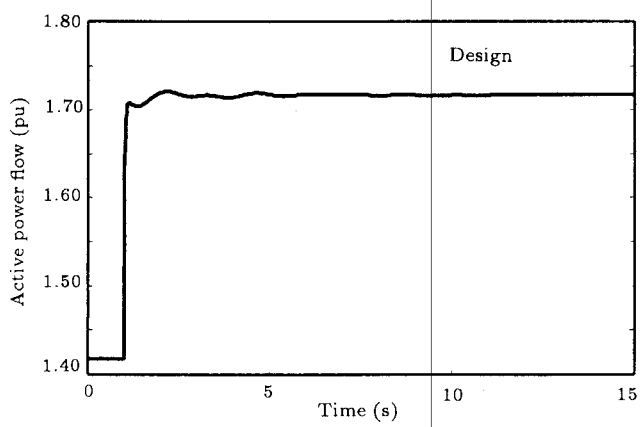

Figure 8. Step response of the system with $PI - P_1$ controller designed.

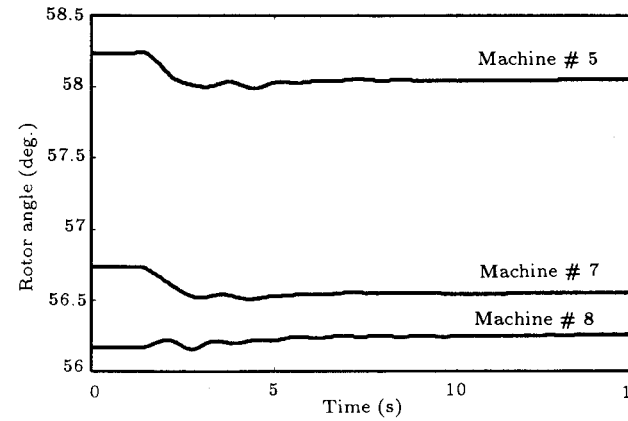

Figure 11. Rotor angle response of the system with $PI - Q_1$ controller installed.

and $K_{IQ_{line2}} = 2.0$. Figures 18 and 19 show the system response.

In all the above cases, satisfactory control performance and closed-loop system stability are achieved by the design of each individual controller. When all controllers are in joint operation, the reference value of each controller is changed again, sequentially, to evaluate control performance and closed-loop system stability. The results are shown in Figures 20 to 27. It can be seen that, in all cases, the closed-loop system stability is lost. It means that when the

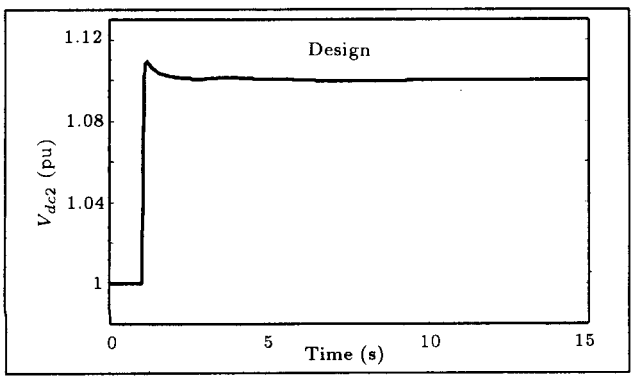

Figure 12. Step response of the system with $PI - V_{dc2}$ controller designed.

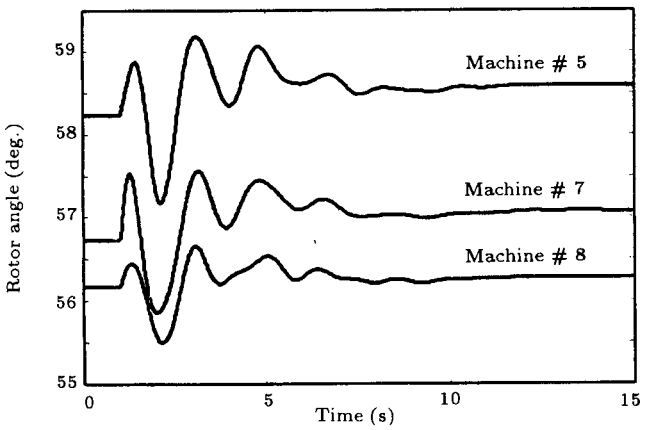

Figure 13. Rotor angle response of the system with $PI - V_{dc2}$ controller installed.

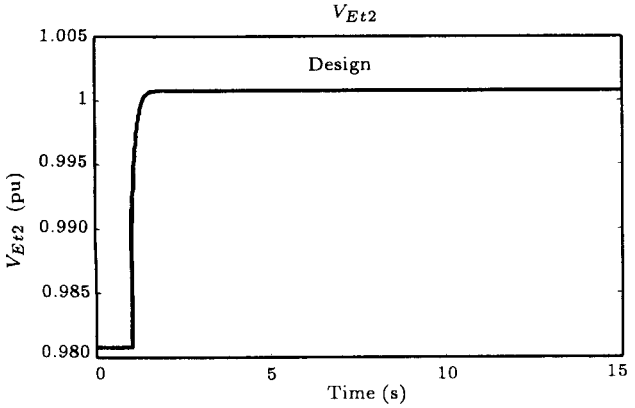

Figure 14. Step response of the system with $PI - V_{Et2}$ controller designed.

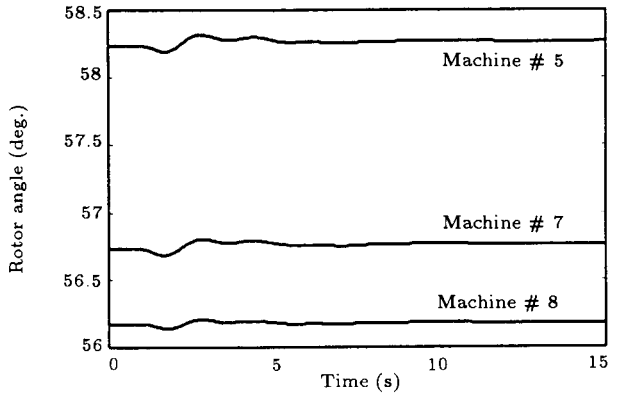

Figure 15. Rotor angle response of the system with $PI - V_{Et2}$ controller installed.

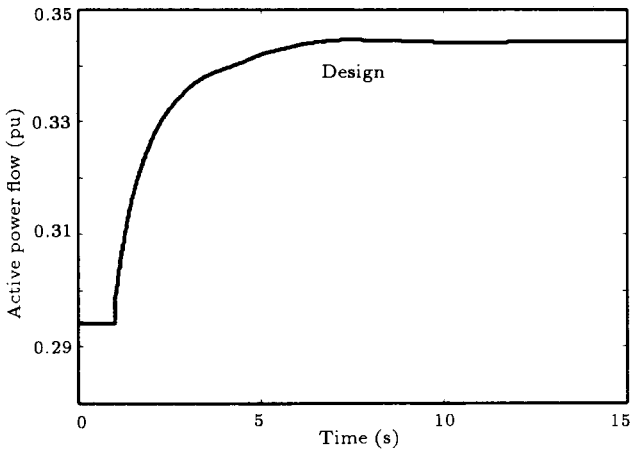

Figure 16. Step response of the system with $PI - P_2$ controller designed.

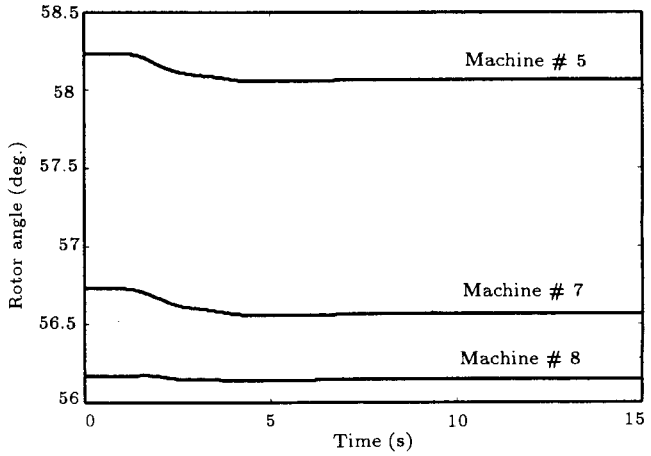

Figure 17. Rotor angle response of the system with $PI - P_2$ controller installed.

PI-controllers are designed as SISO controllers, the interaction between the control channels of different control functions are not considered. Hence, closed-loop system stability cannot be guaranteed when all SISO controllers are put into operation.

In other words, the defect of the SISO design ap-

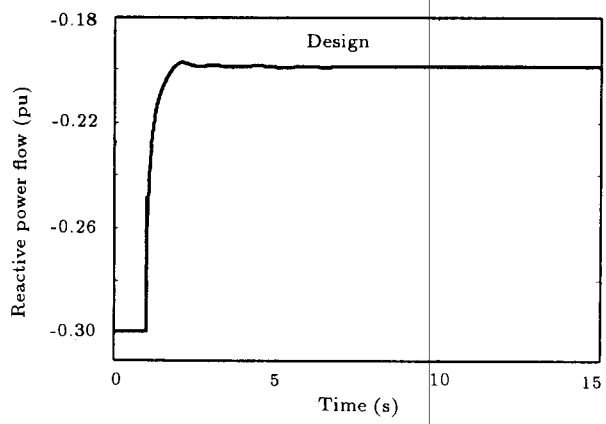

Figure 18. Step response of the system with $PI - Q_2$ controller designed.

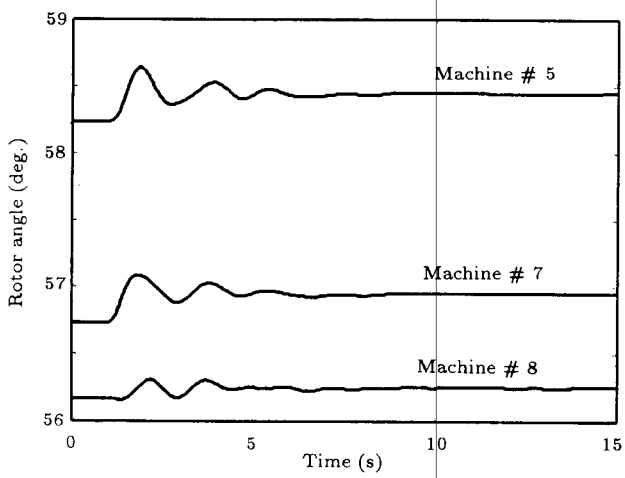

Figure 19. Rotor angle response of the system with $PI - Q_2$ controller installed.

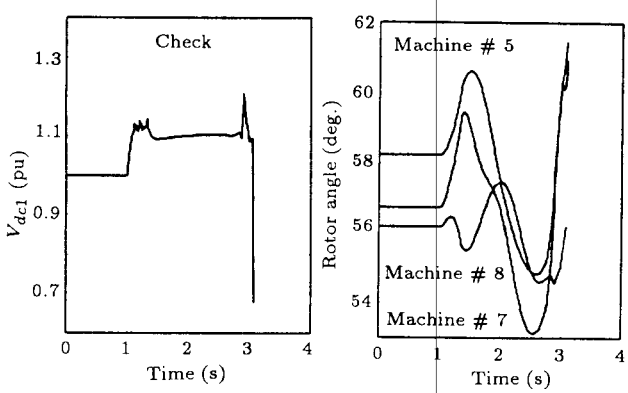

Figure 20. $PI - V_{dc1}$ controller performance and the closed-loop system instability.

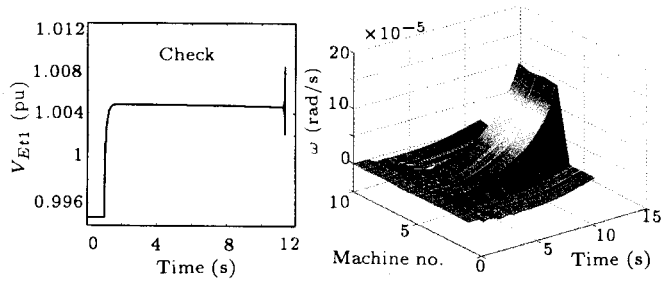

Figure 21. $PI - V_{Et1}$ controller performance and the closed-loop system instability shown by the machine rotor speeds.

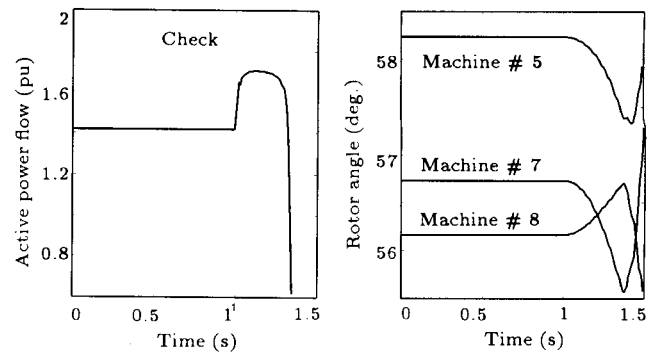

Figure 22. $PI - P_{\text{line1}}$ controller performance and the closed-loop system instability.

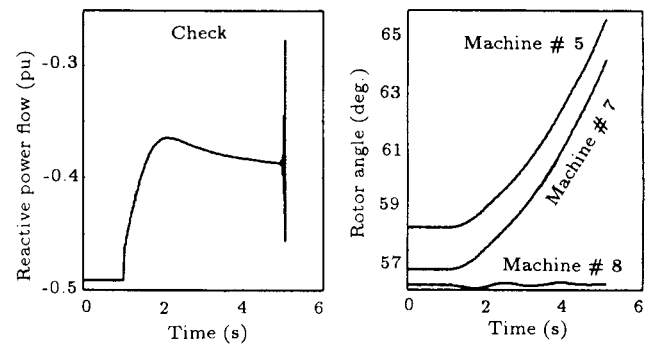

Figure 23. Checking $PI - Q_1$ controller performance and instability of the closed-loop system.

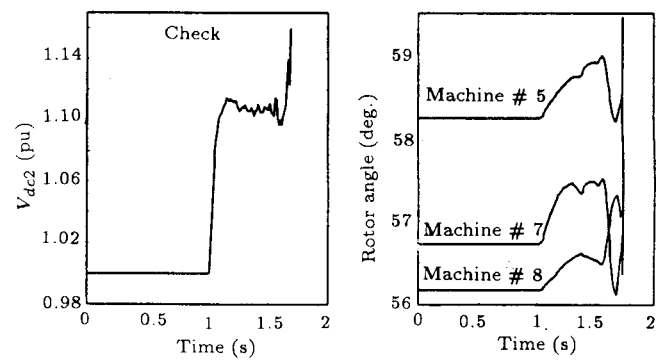

Figure 24. Checking $PI - V_{dc2}$ controller performance and instability of the closed-loop system.

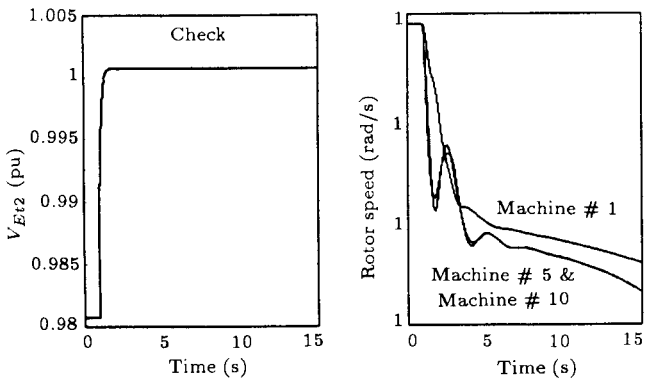

Figure 25. Checking $PI - V_{Et2}$ controller performance and instability of the closed-loop system.

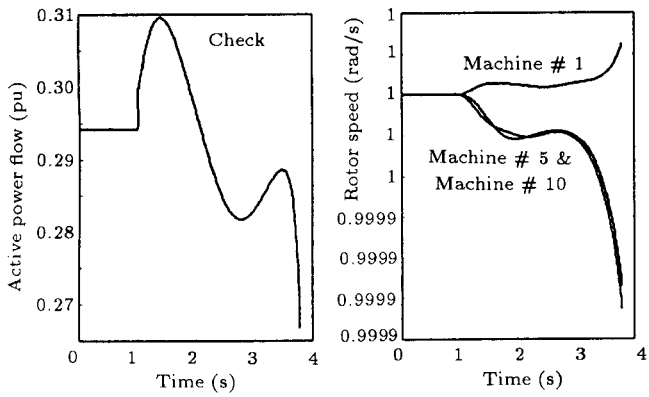

Figure 26. Checking $PI - P_2$ controller performance and instability of the closed-loop system.

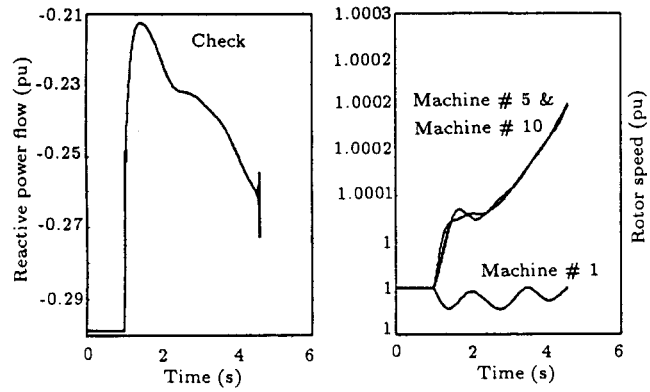

Figure 27. Checking $PI - Q_2$ controller performance and instability of the closed-loop system.

plied above is that when a controller is being designed, the influence of other controllers cannot be considered. Therefore, when those controllers are in joint operation, the control performance of the controller being designed cannot be ensured. This is why multiple SISO controllers cannot be often applied for a multivariable control system. The results presented here for UPFC applications provide clear evidence to this fact.

CONCLUSION

In this paper, a method to embed two UPFCs into a multi-machine power system is presented. The method is then applied to investigate dynamic interaction between multiple UPFC control functions. The study cases confirm that interaction exists not only among different SISO controllers assigned to the same UPFC, but, also, between controllers of different UPFCs. This negative dynamic interaction can cause the instability of the overall closed-loop system. To overcome the interaction of UPFC control functions by some advanced techniques of controller design needs further work in the future. However, multivariable controller design provides a simple solution if a centralized control scheme can be applied.

REFERENCES

1. Gyugyi, L.G. "A unified power flow control concept of flexible AC transmission systems", *IEE Proceedings-Control*, **139**(4), pp 323-333 (July 1992).
2. Gyugyi, L., Rietman, T.R., Edris, A., Schauder, C.D., Torgerson, D.R. and Williams, S.L. "The unified power flow controller: A new approach to power transmission control", *IEEE Transaction on Power Delivery*, **10**(2) (April 1995).
3. Wang, H.F. "Damping function of unified power flow controller", *IEE Pro. Gener. Trans. Distrib.*, **146**(1) (Jan 1999).
4. Mihalic, R. and Zunko, P. "Improvement of transient stability using unified power flow controller", *IEEE Transaction on Power Delivery*, **11**(1) (January 1996).
5. Mishra, S., Dash, P.K. and Panda, G. "TS-fuzzy controller for UPFC in a multi machine power system", *IEE Proc.-Gener. Transm. Distrib.*, **147**(1) (January 2000).
6. Wang, H.F., Jazaeri, M. and Johns, A.T. "Investigation into the dynamic interactions of multifunctional unified power flow controllers", *IEEE Review* (July 2000).
7. Jazaeri, M., Wang, H.F., Johns, A.T. and Ehsan, M. "Unified power flow controller (UPFC), its proposal, research and applications- A survey", *Proceedings of the Universities Power Engineering Conference*, p 175 (2000).
8. Nabavi-Niaki, A. and Iravani, M.R. "Steady-state and dynamic models of unified power flow controller (UPFC) for power system studies", *IEEE Transaction on Power System*, **11**(4) (Nov. 1996).
9. *Modelling of Power Electronics Equipment (FACTS) in Load Flow and Stability Programs*, CIGRE TF 38-01-08.
10. Wang, H.F. "Application of modelling UPFC into multi-machine power systems", *IEE Pro. Gener. Trans. Distrib.*, **146**(3) (May 1999).